



OPEN

Effects of splenectomy on skin inflammation and psoriasis-like phenotype of imiquimod-treated mice

Hiroyo Shinno-Hashimoto^{1,2}, Akifumi Eguchi³, Akemi Sakamoto⁴, Xiayun Wan², Yaeko Hashimoto^{2,5}, Yuko Fujita², Chisato Mori^{3,6}, Masahiko Hatano⁴, Hiroyuki Matsue¹ & Kenji Hashimoto²

Imiquimod (IMQ) is widely used as animal model of psoriasis, a chronic inflammatory skin disorder. Although topical application of IMQ to back skin causes splenomegaly in mice, how the spleen affects the psoriasis-like phenotype of IMQ-treated mice remains unclear. In this study, we analyzed the cellular composition of spleen and measured metabolites in blood of IMQ-treated mice. We also investigated whether splenectomy influences the degree of skin inflammation and pathology in IMQ-treated mice. Flow cytometry showed that the numbers of CD11b⁺Ly6c⁺ neutrophils, Ter119⁺ proerythroblasts, B220⁺ B cells, F4/80⁺ macrophages, and CD11c⁺ dendritic cells in the spleen were significantly higher in IMQ-treated mice compared to control mice. An untargeted metabolomics analysis of blood identified 14 metabolites, including taurine and 2,6-dihydroxybenzoic acid, whose levels distinguished the two groups. The composition of cells in the spleen and blood metabolites positively correlated with the weight of the spleen. However, splenectomy did not affect IMQ-induced psoriasis-like phenotypes compared with sham-operated mice, although splenectomy increased the expression of interleukin-17A mRNA in the skin of IMQ-treated mice. These data suggest that the spleen does not play a direct role in the development of psoriasis-like phenotype on skin of IMQ-treated mice, though IMQ causes splenomegaly.

Psoriasis is an autoimmune disease that causes raised plaques and scaly patches on the skin. Yet psoriasis-induced inflammation could harm other organs: patients with psoriasis have a high risk for systemic comorbidities, including psoriatic arthritis, inflammatory bowel diseases, obesity, diabetes, and cardiovascular diseases. For example, approximately 30% of patients with psoriasis develop psoriatic arthritis¹. Data from immunological and genetic studies suggest that interleukin-17 (IL-17) and IL-23 govern crosstalk between the innate and adaptive immune systems in a feed-forward amplification of psoriasis inflammation^{2–4}. Although excessive activation of the immune system plays a crucial role in the pathogenesis of psoriasis, the precise mechanisms underlying this disease remain elusive^{2–8}.

Imiquimod (IMQ), a Toll-like receptor 7 agonist, has been used as a rodent model of psoriasis^{9,10}. It is also suggested that the skin serves as a peripheral neuroendocrine tissue^{11,12}. Topical application of IMQ to back skin causes splenomegaly in rodents^{9,13–17}. Given the key role of immune system in the spleen^{18–21}, the spleen may play a role in psoriasis-like skin inflammation of IMQ-treated mice by modulating the immune system. However, how the spleen and splenectomy contribute to the psoriasis-like phenotype of IMQ-treated mice is unknown.

The present study investigated how the spleen impacts the psoriasis-like phenotype of IMQ-treated mice. First, we analyzed the cellular composition in the spleen of control and IMQ-treated mice by using flow cytometry. Then we examined correlations between spleen weight and cellular composition in the spleen. Second, we

¹Department of Dermatology, Chiba University Graduate School of Medicine, Chiba 260-8670, Japan. ²Division of Clinical Neuroscience, Chiba University Center for Forensic Mental Health, Chiba 260-8670, Japan. ³Department of Sustainable Health Science, Center for Preventive Medical Sciences, Chiba University, Chiba 263-8522, Japan. ⁴Department of Biomedical Science, Chiba University Graduate School of Medicine, Chiba 260-8670, Japan. ⁵Department of Respiratory, Chiba University Graduate School of Medicine, Chiba 260-8670, Japan. ⁶Department of Bioenvironmental Medicine, Graduate School of Medicine, Chiba University, Chiba 260-8670, Japan. ✉email: hiroyo.h@chiba-u.jp; hashimoto@faculty.chiba-u.jp

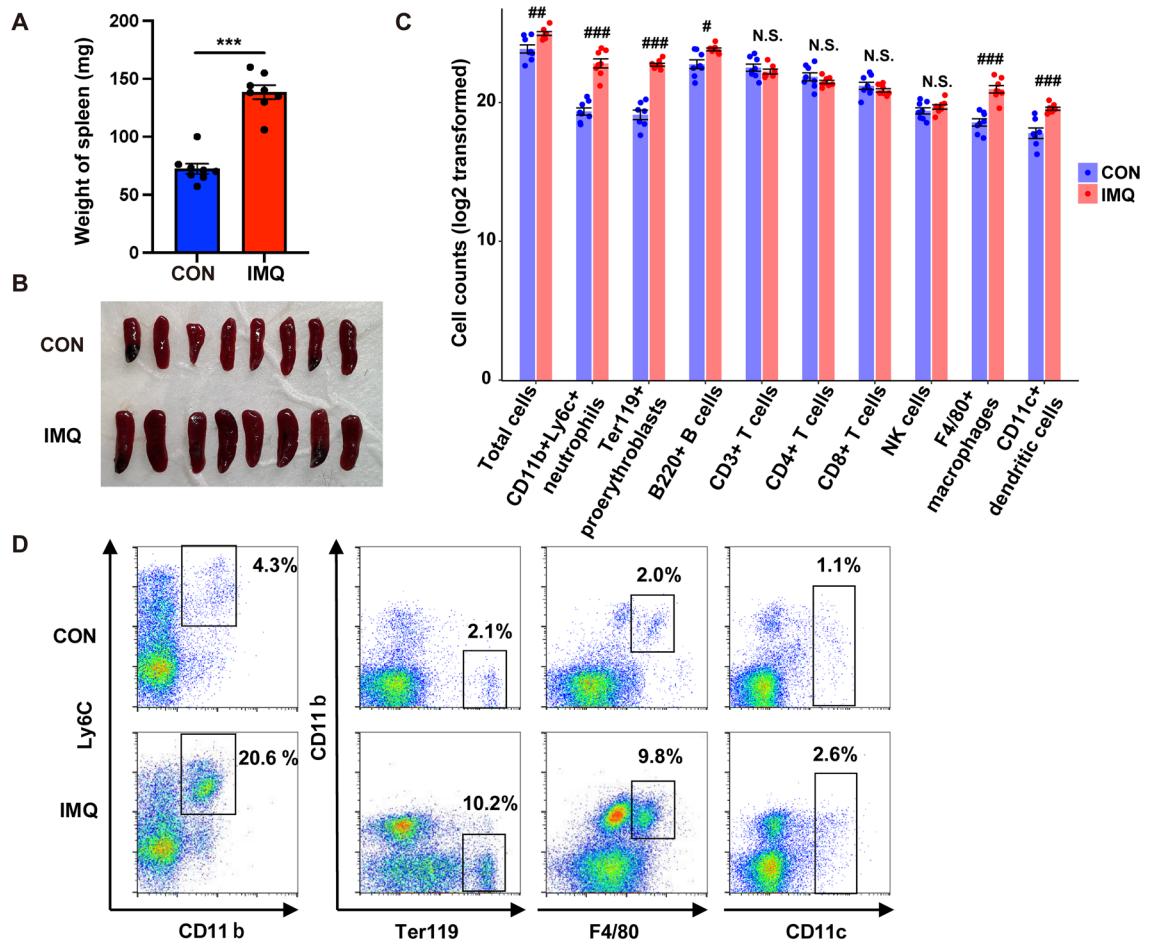


Figure 1. Effects of IMQ on weight and cell populations of spleen. **(A):** Spleen weight (Student *t*-test: *df* = 14, *t* = −9.017, *P* = 0.000). **(B):** The photos of spleen from the control group and IMQ group. **(C):** FACS analysis of spleen samples from the two groups. Log₂ transformed data of the number of total cells and each cell type. Total cells (Mann-Whitney test: *U* = 7, FDR-corrected *P* = 0.0079), CD11b⁺Ly6c⁺ neutrophils (Mann-Whitney test: *U* = 0, FDR-corrected *P* = 0.0005), Ter119⁺ proerythroblasts (Mann-Whitney test: *U* = 0, FDR-corrected *P* = 0.0006), B220⁺ B cells (Mann-Whitney test: *U* = 8, FDR-corrected *P* = 0.0105), CD3⁺ T cells (Mann-Whitney test: *U* = 19, FDR-corrected *P* = 0.2073), CD4⁺ T cells (Mann-Whitney test: *U* = 22, FDR-corrected *P* = 0.2073), CD8⁺ T cells (Mann-Whitney test: *U* = 19, FDR-corrected *P* = 0.1605), NK1.1⁺ NK cells (Mann-Whitney test: *U* = 22.5, FDR-corrected *P* = 0.2073), F4/80⁺ macrophages (Mann-Whitney test: *U* = 0, FDR-corrected *P* = 0.0005), CD11c⁺ DCs (Mann-Whitney test: *U* = 1, FDR-corrected *P* = 0.0009). Data are shown as mean ± SEM (*n* = 8). One data of Ter119⁺ proerythroblasts and CD11c⁺ DCs in the control group and one data of CD3⁺ T cells in the IMQ group were missing because of technical problems. #*P* (FDR-corrected) < 0.05, ##*P* (FDR-corrected) < 0.01, ###*P* (FDR-corrected) < 0.001. NS: not significant. **(D):** The representative FACS data of CD11b⁺Ly6c⁺ neutrophils, Ter119⁺ proerythroblasts, F4/80⁺ macrophages, and CD11c⁺ DCs in the spleen of control mice and IMQ-treated mice.

performed non-targeted metabolome analysis of blood samples from the two groups and examined correlations between spleen weight and blood metabolites. Finally, we determined whether splenectomy could affect psoriasis-like phenotype and skin inflammation in IMQ-treated mice.

Results

Effects of IMQ on weight and cell populations of spleen. Topical application of IMQ caused significantly increased spleen weight in IMQ-treated mice compared to control mice (Fig. 1A,B), consistent with our previous report²². The number of total cells of IMQ-treated mice was also significantly higher than those of control mice (Fig. 1C). Spleen cells were analyzed for the percentage and the number of CD11b⁺Ly6c⁺ neutrophils, Ter119⁺ proerythroblasts, B220⁺ B cells, CD3⁺ T cells, CD4⁺ T cells, CD8⁺ T cells, NK1.1⁺ natural killer (NK) cells, F4/80⁺ macrophages, and CD11c⁺ dendritic cells (DCs). The number of neutrophils, proerythroblasts, B cells, macrophages, and DCs in the spleen of IMQ-treated mice was significantly higher than those of control mice (Fig. 1C,D). In contrast, there were no differences in the number of T cells (CD3⁺, CD4⁺, and CD8⁺) and NK cells (Fig. 1C).

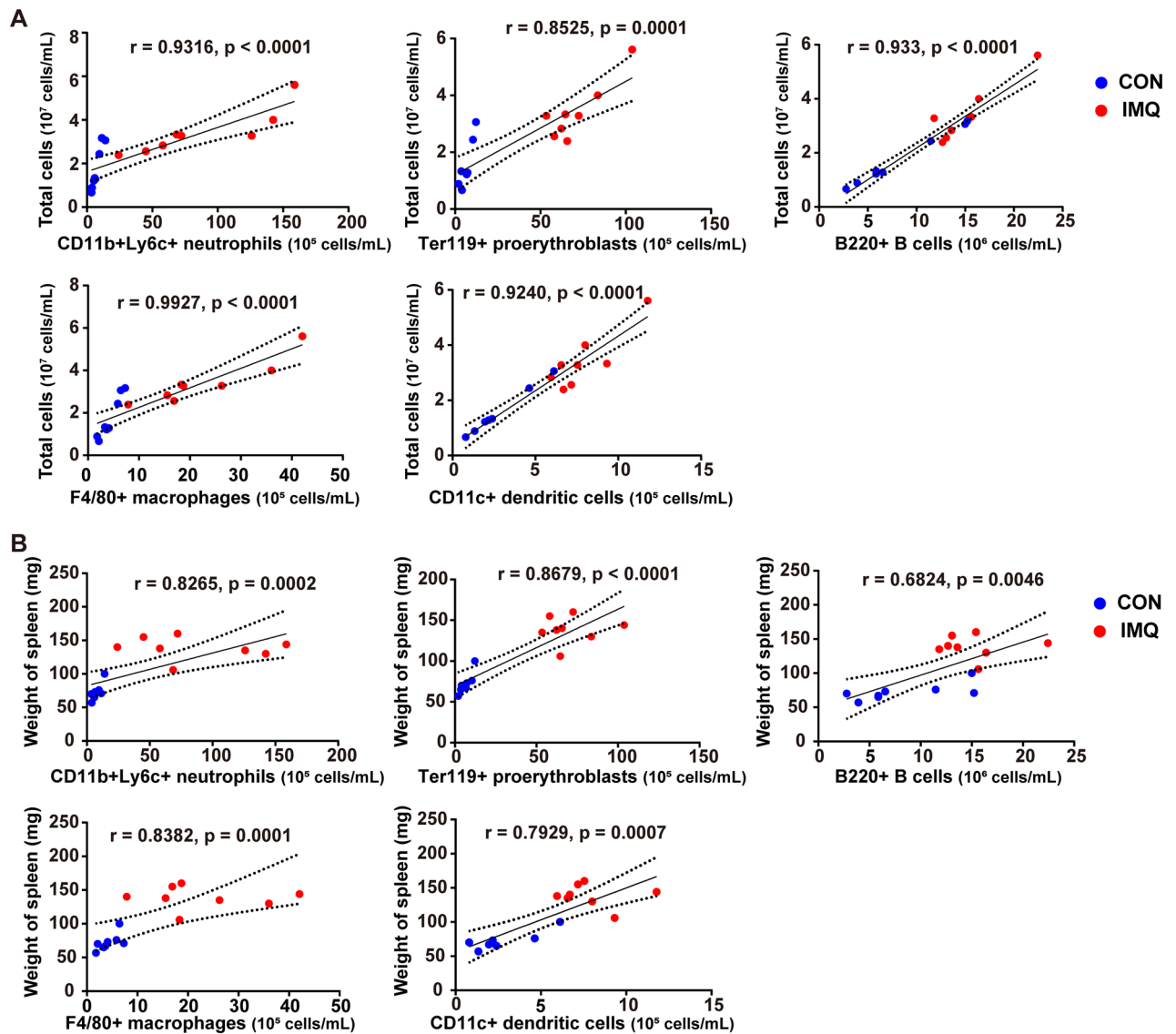
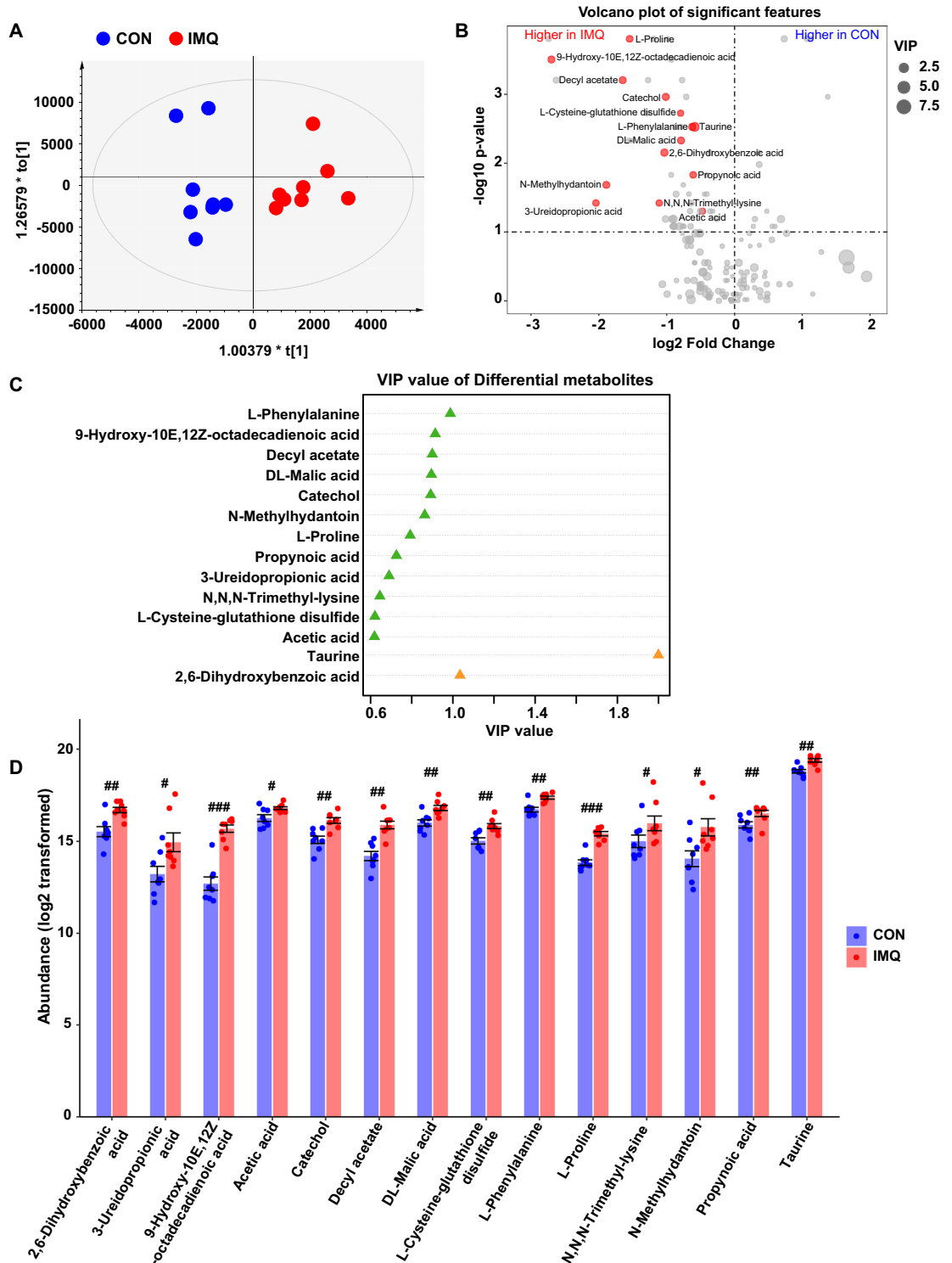


Figure 2. Correlations between the number of total splenic cells (or spleen weight) and the number of the splenic cell types. (A): The correlations between the number of total splenic cells and the number of the splenic cell types whose amount significantly increased in IMQ group. (B): The correlations between the weight of spleen and the number of the splenic cell types whose amount significantly increased in IMQ group. The values represent the mean \pm SEM ($n = 8$).

The total number of cells in the spleen positively correlated with the cell types (i.e., neutrophils, proerythroblasts, B cells, macrophages, and DCs) in the two groups (Fig. 2A). Moreover, the weight of spleen positively correlated with the cell types (i.e., neutrophils, proerythroblasts, B cells, macrophages, and DCs) in the two groups (Fig. 2B).

Non-targeted metabolomic profiling of plasma. We performed non-targeted metabolomic profiling of plasma samples from IMQ-treated mice and control mice. After quality control and removal of low-abundance peaks, a subset of 173 metabolites was annotated. Orthogonal partial least squares discriminant analysis (OPLS-DA) revealed that the metabolic composition of IMQ group was significantly different from that of the control group (Fig. 3A). After thresholding (variable importance in the projection [VIP] value > 0.6 , Wilcoxon rank p -value < 0.05), we identified 14 metabolites altered between the two groups (Fig. 3B). Among the 14 metabolites, taurine and 2,6-dihydroxybenzoic acid had VIP > 1.0 (Fig. 3C). The fourteen metabolites that increased in the IMQ group were taurine, 2,6-dihydroxybenzoic acid, L-phenylalanine, 9-hydroxy-10E,12Z-octadecadienoic acid, decyl acetate, DL-malic acid, catechol, *N*-methylhydantoin, L-proline, propynoic acid, 3-ureidopropionic acid, *N,N,N*-trimethyl-L-lysine, L-cysteine-glutathione disulfide, and acetic acid (Fig. 3D).

Associations between spleen cells, spleen weight, and plasma metabolites. Spearman correlation analysis was used to quantify the correlations between the spleen cell types, spleen weight, and the fourteen



differential metabolites of plasma. Several cell types and spleen weight were significantly correlated with the plasma metabolites in the two groups (Fig. 4A). The cell types such as total cells, neutrophils, and macrophages were positively associated with plasma metabolites except *N,N,N*-trimethyl-lysine. The other cell types (B cells, proerythroblasts, and DCs) were positively associated with several metabolites. Spleen weight was also positively associated with plasma metabolites except *N,N,N*-trimethyl-lysine (Fig. 4A).

Spearman correlation was also used to determine if IMQ-related cell types in the spleen and plasma metabolites contribute to splenomegaly. The cell types in the spleen and plasma metabolites differentially abundant in the two groups showed more associations with spleen weight (Fig. 4B). Interestingly, neutrophils in the spleen were positively correlated with spleen weight and plasma metabolites (Fig. 4B).

◀ **Figure 3.** Effects of IMQ on metabolites of plasma. (A): Scatter plot of murine plasma metabolites based on orthogonal partial least square discriminant analysis (OPLS-DA) between IMQ group and control group. (B): Volcano plot shows the differential metabolites between the two groups. The X-axis indicates the log₂-transformed plasma metabolite abundance of fold change, and the Y-axis indicates the -log₁₀-transformed *P* value using the Wilcoxon rank sum test. Horizontal lines indicate *P* < 0.05. Increased or decreased metabolites are marked in red and blue, respectively. The size of the dot represents the size of the VIP value. Metabolites with *P* < 0.05 and VIP > 0.6 are mentioned in text. (C): VIP value of the differential metabolites between the two groups. (D): Log₂ transformed data of the abundance of the differential plasma metabolites. 2,6-dihydroxybenzoic acid (Mann-Whitney test: *U* = 7, FDR-corrected *P* = 0.0047), 3-ureidopropionic acid (Mann-Whitney test: *U* = 12, FDR-corrected *P* = 0.0177), 9-hydroxy-10E,12Z-octadecadienoic acid (Mann-Whitney test: *U* = 1, FDR-corrected *P* = 0.0009), acetic acid (Mann-Whitney test: *U* = 13, FDR-corrected *P* = 0.00216), catechol (Mann-Whitney test: *U* = 3, FDR-corrected *P* = 0.0016), decyl acetate (Mann-Whitney test: *U* = 2, FDR-corrected *P* = 0.0013), DL-malic acid (Mann-Whitney test: *U* = 6, FDR-corrected *P* = 0.0035), L-cysteine-glutathione disulfide (Mann-Whitney test: *U* = 4, FDR-corrected *P* = 0.0023), L-phenylalanine (Mann-Whitney test: *U* = 5, FDR-corrected *P* = 0.0026), L-proline (Mann-Whitney test: *U* = 0, FDR-corrected *P* = 0.0009), *N,N,N*-trimethyl-lysine (Mann-Whitney test: *U* = 12, FDR-corrected *P* = 0.0177), *N*-methylhydantoin (Mann-Whitney test: *U* = 10, FDR-corrected *P* = 0.0114), propynoic acid (Mann-Whitney test: *U* = 9, FDR-corrected *P* = 0.0089), taurine (Mann-Whitney test: *U* = 5, FDR-corrected *P* = 0.0026). Data are shown as mean ± SEM (*n* = 8). **P* (FDR-corrected) < 0.05, ***P* (FDR-corrected) < 0.01, ****P* (FDR-corrected) < 0.001.

Effect of splenectomy on skin inflammation and body weight changes in IMQ-treated mice. Topical application of IMQ induced psoriasis-like dermatitis in both sham group and splenectomy group (Fig. 5A). Representative hematoxylin and eosin staining of the back skin showed acanthosis and parakeratosis with microabscess in the two groups (Fig. 5B). The cumulative scores of the sham-IMQ group and splenectomy-IMQ group were not significantly different (Fig. 5C).

Next, we measured the gene expression levels of IL-17A and IL-23A in the skin. The mRNA levels of IL-17A and IL-23A in the IMQ group were higher than those of the control group (Fig. 5D). Expression of IL-17A mRNA in the splenectomy-IMQ group was significantly higher than that of sham-IMQ group, whereas the expression of IL-23A mRNA was not different between the sham-IMQ group and splenectomy-IMQ group (Fig. 5D). There were also no changes in the body weight between sham group and splenectomy group in both of IMQ group and control group (Fig. 5E).

Discussion

This is the first study to show how the spleen contributes to psoriasis-like phenotypes in IMQ-treated mice. Indeed, topical application of IMQ significantly increased infiltration of immune cells such as neutrophils, DCs, macrophages, and B cells in the spleen, which agrees with previous studies. These cell types correlated with spleen weight, which also correlated with higher levels of 14 metabolites in the plasma of IMQ-treated mice; taurine and 2,6-dihydroxybenzoic acid had especially high VIP values. These metabolites likely contribute to splenomegaly upon IMQ application. Finally, we showed that splenectomy does not affect a psoriasis-like phenotype on the skin of IMQ-treated mice but could potentiate IMQ-induced increases in IL-17A mRNA in the skin.

Neutrophils, proerythroblasts, B cells, macrophages, and DCs significantly enlarged the IMQ-treated spleen; their cell compartments positively correlated with spleen weight. Interestingly, the percentage of B cells in the spleen did not change between the control group and IMQ-treated group. Previously, percentages of macrophages and DCs increased and the percentage of T cells (both CD4⁺ and CD8⁺) decreased in an IMQ-treated group⁹, consistent with the current data. Topical treatment with IMQ likely induces inflammation, and increased numbers of immune cells cause splenomegaly.

The longitudinal diameter of the spleen and the duration of psoriasis were correlated in a previous study of 79 psoriatic patients²³, suggesting that increased diameter of the spleen in psoriatic patients with long-term illness is related to chronic inflammation. Future clinical studies are needed to confirm the role of spleen in the pathogenesis of psoriasis²⁴.

Non-targeted metabolomics profiling identified 14 metabolites whose levels were significantly different between the IMQ-treated group and the control group. Taurine and 2,6-dihydroxybenzoic acid had the highest VIP values, indicating that they contributed the most to the separation between groups. Taurine plays an important role in inflammation associated with oxidative stress^{25,26} and may play a pathological role in psoriasis given its higher levels in blood from patients with psoriasis when compared to healthy controls²⁷. Taurine reduced blood levels of IL-6 in patients with traumatic brain injury in a recent randomized double-blind controlled trial²⁸. Taurine's anti-inflammatory actions^{25,26} in the blood of IMQ-treated mice may compensate for IMQ-induced inflammation in the body. Further studies should explore how taurine affects spleen size in IMQ-treated mice. The function of 2,6-dihydroxybenzoic acid remains unclear but is likely anti-inflammatory²⁹. Higher levels of 2,6-dihydroxybenzoic acid in the blood of IMQ-treated mice may also compensate for IMQ-induced inflammation in the body. These metabolites should be targeted in future studies on splenomegaly of IMQ-treated mice.

Spleen enlargement is linked to systemic inflammation³⁰. For example, we reported splenomegaly in mice treated with lipopolysaccharide (LPS), and there were positive correlations between spleen weight and blood levels of pro-inflammatory cytokines (i.e., IL-6, tumor necrosis factor-α)^{31–33}. A chronic social defeat stress (CSDS) model revealed that the spleen weight of susceptible mice with depression-like behaviors was higher than that

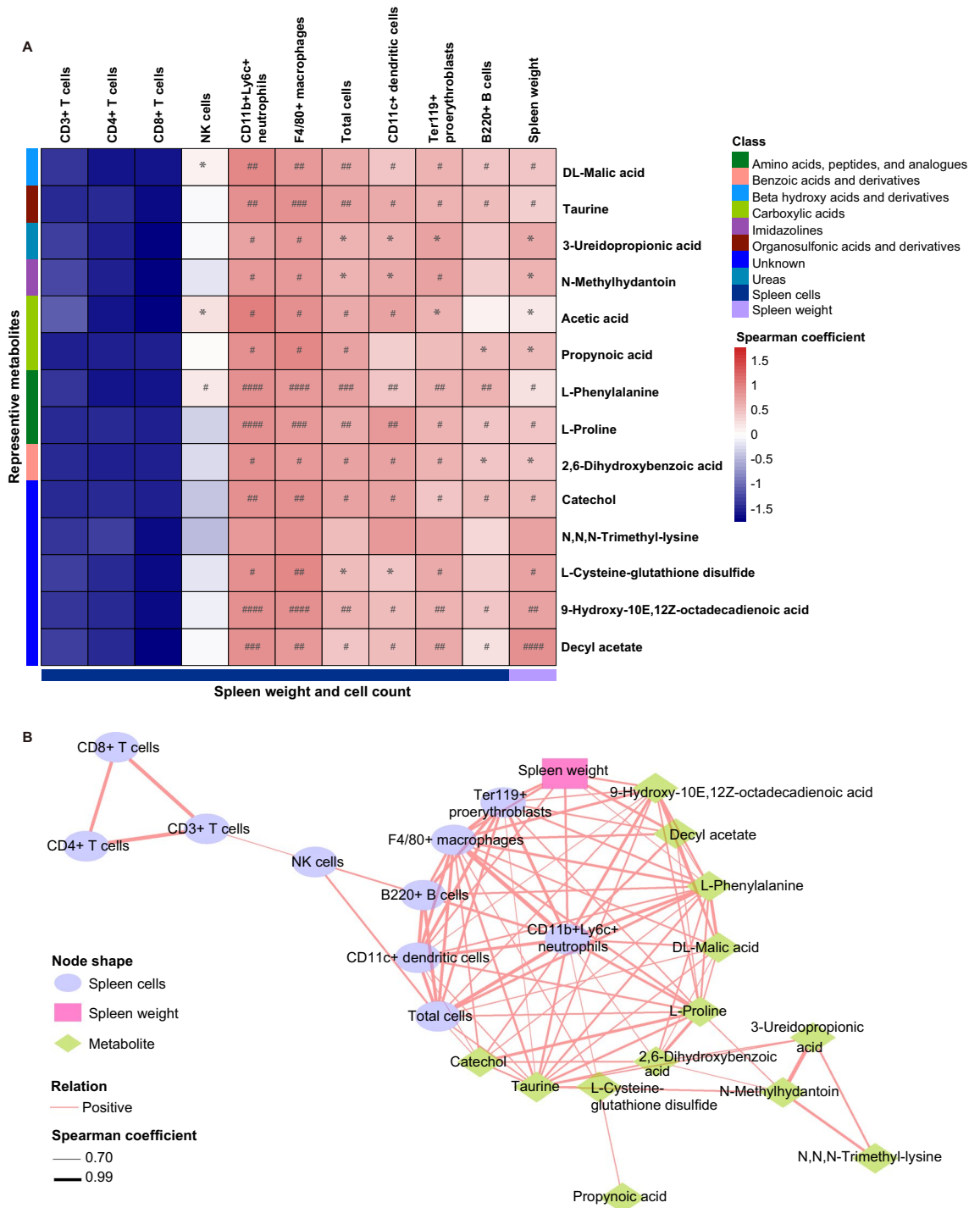


Figure 4. Associations among spleen cell types, spleen weight and the metabolites of plasma samples. **(A):** Heatmap of Spearman rank correlation coefficients between counts of splenic cell types or spleen weight and the metabolites of plasma samples. * $P < 0.05$ and FDR-corrected $P > 0.05$, * P (FDR-corrected) < 0.05 , ** P (FDR-corrected) < 0.01 , *** P (FDR-corrected) < 0.001 , **** P (FDR-corrected) < 0.0001 . **(B):** Correlation network analysis reveals the associations among counts of spleen cell types, spleen weight and the plasma metabolites. Each node shape represents spleen cell types, spleen weight or plasma metabolites, respectively. The pink lines connecting the nodes indicate positive correlation and the line weight indicates spearman correlation coefficient. We created the network using Cytoscape software 3.8.0. (<https://cytoscape.org>).

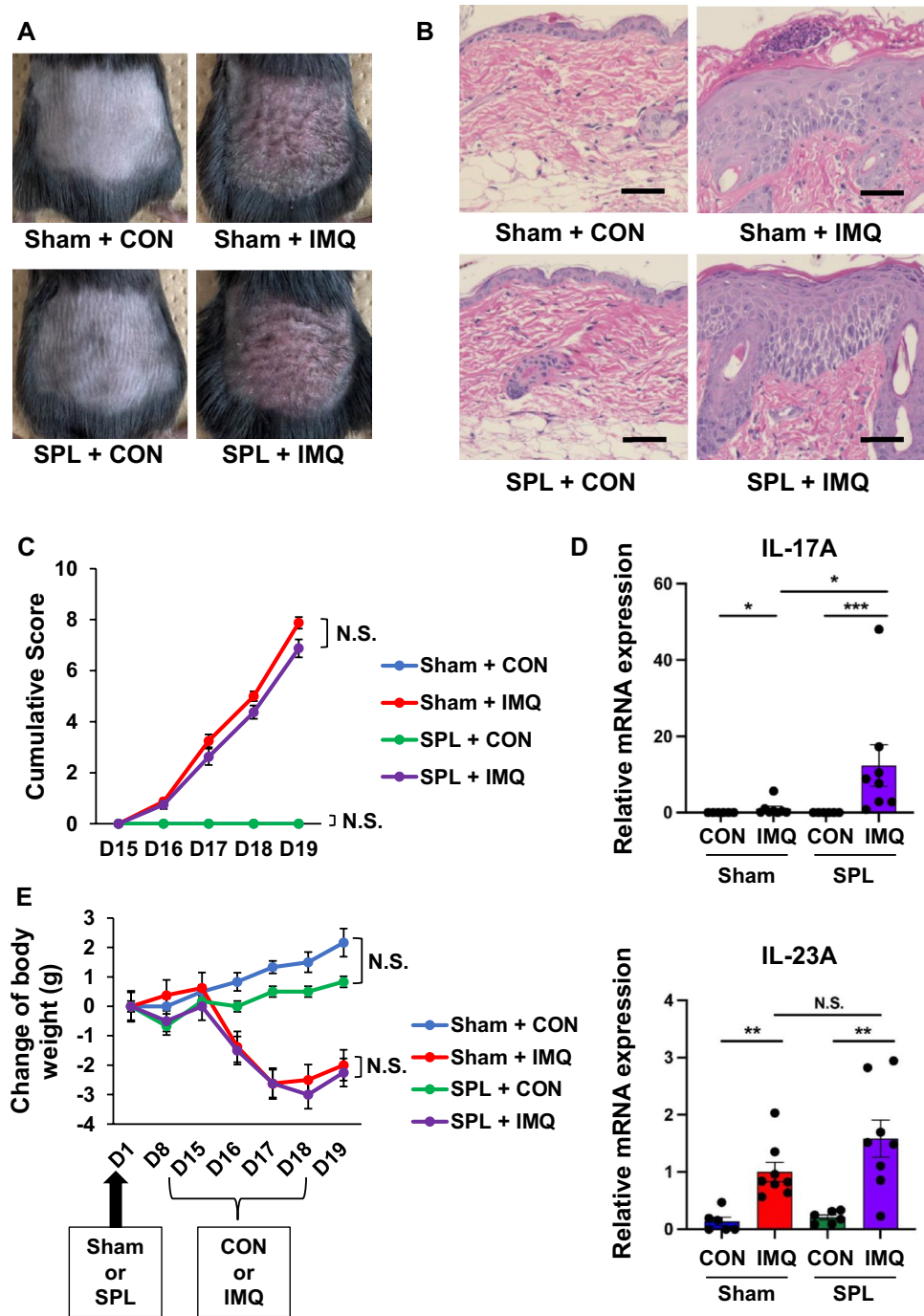


Figure 5. Effect of splenectomy on the skin inflammation and body weight changes in IMQ-treated mice. (A): Mice were treated topically with 5% IMQ cream or control cream on the shaved back for four days two weeks after sham or splenectomy. The representative photos of back skin from the four groups. (B): HE staining of the back skin. Scale bar = 50 μ m. (C): Cumulative skin scores from day 15 to day 19. Day 15 (Kruskal–Wallis test: $H=0.000, P=1.000$), day 16 (Kruskal–Wallis test: $H=17.792, P=0.000$), day 17 (Kruskal–Wallis test: $H=22.840, P=0.000$), day 18 (Kruskal–Wallis test: $H=23.619, P=0.000$), day 19 (Kruskal–Wallis test: $H=23.459, P=0.000$). Scores of sham + control group and splenectomy + control group are 0 from D15 to D19. (D): Relative mRNA expression levels of IL-17A and IL23-A in murine back skin. IL-17A mRNA (Kruskal–Wallis test: $H=23.332, P=0.000$), IL-23A mRNA (Kruskal–Wallis test: $H=19.302, P=0.000$). * $P<0.05$, ** $P<0.01$, *** $P<0.001$. (E): Change of body weight. Day 1 (Kruskal–Wallis test: $H=0.000, P=1.000$), day 8 (Kruskal–Wallis test: $H=7.641, P=0.054$), day 15 (Kruskal–Wallis test: $H=2.022, P=0.568$), day 16 (Kruskal–Wallis test: $H=10.921, P=0.012$), day 17 (Kruskal–Wallis test: $H=20.213, P=0.000$), day 18 (Kruskal–Wallis test: $H=21.758, P=0.000$), day 19 (Kruskal–Wallis test: $H=20.287, P=0.000$). The values represent the mean \pm SEM. (n = 6 or 8). NS: not significant. SPL: Splenectomy.

of control mice and CSDS-resilient mice³⁴. Collectively, it is likely that LPS- (or CSDS)-induced splenomegaly is associated with systemic inflammation^{31–36}.

Considering the spleen's key role in the immune system^{18–21}, we investigated how splenectomy affects psoriasis-like pathology and skin inflammation of IMQ-treated mice. Unexpectedly, splenectomy did not change the psoriasis-like phenotype in IMQ-treated mice. However, we found that splenectomy significantly enhanced IL-17A mRNA in the skin of IMQ-treated mice compared to sham-operated mice. The spleen may not directly impact the psoriasis-like phenotype of IMQ-treated mice, but it does cause splenomegaly.

This study has one limitation. In this study, we used 5% IMQ cream (Beselna cream). The full list of excipients is isostearic acid, benzyl alcohol, cetyl alcohol, stearyl alcohol, white soft paraffin, polysorbate 60, sorbitan stearate, glycerol, methyl hydroxybenzoate, propyl hydroxybenzoate, xanthan gum, and purified water. Walter et al.³⁷ reported that isostearic acid, a major component, could promote inflammasome activation in cultured keratinocytes, and that it increased the expression of inflammatory cytokines *in vivo*. These data suggest that isostearic acid may contribute to the observed effects of Beselna cream used in this study^{37,38}. In this study, we did not examine the effects of isostearic acid on spleen function since the company did not disclose the detailed information of excipients including isostearic acid. Further study is needed to investigate the effects of isostearic acid on spleen functions.

In conclusion, this study highlighted the key role of the spleen in chronic inflammation of IMQ-treated mice. The numbers of neutrophils, proerythroblasts, B cells, macrophages, and DCs in the spleen significantly increased, which correlated with higher spleen weight. Metabolomics profiling also revealed metabolites whose roles in psoriasis pathogenesis can be studied further. However, splenectomy did not affect psoriasis-like phenotypes in IMQ-treated mice. Although the spleen may not play a major role in psoriasis-like phenotypes in IMQ-treated mice, topical application of IMQ to back skin causes splenomegaly.

Materials and methods

Animals. Nine-week-old female C57BL/6 mice (weighing 18–21 g, n = 16, Japan SLC Inc., Hamamatsu, Shizuoka, Japan) were used in Experiment 1. Seven-week-old female C57BL/6 mice (weighing 18–21 g, n = 28, Japan SLC Inc., Hamamatsu, Shizuoka, Japan) were used in Experiment 2. Mice were housed (3–4 per cage) under a 12-h/12-h light/dark cycle (lights on between 07:00 and 19:00), with *ad libitum* access to food (CE-2; CLEA Japan, Inc., Tokyo, Japan) and water. The experimental protocol was approved by the Chiba University Institutional Animal Care and Use Committee (Permission number: 2–433). All procedures were performed in accordance with the relevant guidelines and regulations, and the study complied with ARRIVE (Animal Research: Reporting of In Vivo Experiments) guidelines. All efforts were made to minimize animal suffering²².

IMQ treatment. The shaved back skin of mice was treated with 62.5 mg of 5% IMQ cream (Beselna cream; Mochida Pharmaceutical Co., Tokyo, Japan) daily for four consecutive days as previously described²². Control mice were treated similarly with 62.5 mg of white petrolatum (Maruishi Pharmaceutical Co., Osaka, Japan).

Splenectomy. Splenectomy (or sham) surgery was performed under continuous isoflurane inhalation anesthesia as previously described³⁹. Briefly, the mice were anesthetized with 3% isoflurane through an inhalation anesthesia apparatus (KN-1071NARCOBIT-E; Natsume Seisakusho, Tokyo, Japan). In the splenectomy group, each mouse was maintained in a right lateral recumbent position, and an approximately 1-cm incision was made from the abdominal wall under the left costal margin. The skin was dissected, and subcutaneous, muscle, and fascia layers were removed individually until the spleen was exposed. The peripheral ligament of the spleen was separated, associated blood vessels and nerves were ligatured using 6–0 silk sutures, and the spleen was removed by transecting the blood vessels distal to the ligature. Abdominal muscles and the skin incision were closed sequentially using 4–0 silk sutures. The abdominal wall was similarly opened during sham surgery, and the wall was closed immediately after identifying the spleen³⁹. In this study, we did not use opioid and/or non-steroidal anti-inflammatory drugs for pain management after surgery.

Sample collection. *Experiment 1.* After IMQ treatment for four consecutive days, the skin, spleen, and blood samples were collected on day 5.

Experiment 2. Splenectomy or sham was carried out on day 1. Mice were treated with IMQ from day 15 to day 18, and skin samples were collected on day 19. The clinical skin score was measured from day 15 to day 19. The degree of skin inflammation was assessed with a cumulative disease severity score, similar to the human Psoriasis Area and Severity Index but without considering the area. Erythema, scaling, and thickening were scored independently from 0 to 4: 0, none; 1, slight; 2, moderate; 3, marked; 4, very marked. The single scores were summed; the highest possible score is 12⁹.

Fluorescence activated cell sorting analysis of spleen samples. Mouse spleen tissues were mashed and passed through a 100- μ m mesh to prepare a single cell suspension and treated with lysis buffer (0.155 M ammonium chloride, 0.1 M disodium EDTA, 0.01 M potassium bicarbonate) to lyse erythrocytes. Spleen cells were suspended and counted using an automated cell counter (BIO-RAD, Alfred Nobel Drive, CA) prior to fluorescence activated cell sorting (FACS) analysis. We stained 10⁶ cells with various monoclonal antibodies against cell surface antigens for 30 min at 4 °C and then washed them with an FACS buffer [3% fetal calf serum (FCS), 0.04% NaN₃ in phosphate-buffered saline]. Cells were resuspended with 0.4 μ g/ml propidium iodine (cat# P-170; Sigma) containing FACS buffer. The following antibodies were used: anti CD11b-PE (\times 400 diluted using

FACS buffer, cat# 553,312: BD Bioscience, Franklin Lakes, NJ), anti Ly6c-FITC ($\times 100$, cat# 553,104: BD Bioscience), anti B220-PE ($\times 200$, cat# 553,309: BD Bioscience), anti CD8alpha-allophycocyanin ($\times 100$, cat# 553,035: BD Bioscience), anti NK1.1-PE ($\times 100$, cat# 553,165: BD Bioscience), anti CD11c-PE ($\times 100$, cat# 557,401: BD Bioscience), anti Ter119-PE ($\times 40$, cat# 12-5921-83: eBioscience, San Diego, CA), anti CD4-allophycocyanin ($\times 100$, cat# 17-0042-82: eBioscience, San Diego, CA), anti F4/80-PE ($\times 40$, cat# 12-4801-80: Invitrogen), and anti CD3-FITC ($\times 40$, cat# 100,305: BioLegend, San Diego, CA). The stained cells were analyzed using FACS-CantII and FlowJo software (BD Bioscience).

Untargeted metabolomics analysis of plasma samples. Untargeted metabolomics analysis was performed using an ExionLC AD UPLC system (SCIEX, Tokyo, Japan) interfaced with an X500R LC-QToFMS system (SCIEX, Tokyo, Japan) with electrospray ionization (ESI) operating in positive and negative ionization mode, as previous reported^{40,41}. First, 100 μL of methanol containing internal standards (100 μM *N,N*-diethyl-2-phenylacetamide and *d*-camphor-10-sulfonic acid) was added to the plasma samples (100 μL), and then samples were centrifuged at 14,000 \times rpm for 5 min. After centrifugation, the supernatant was transferred to an Amicon® Ultra-0.5 3 kDa filter column (Merck Millipore, Tokyo, Japan) and centrifuged at 14,000 \times rpm for 1 h. The filtrate was transferred to glass vials for subsequent analysis.

The metabolomics data was analyzed with Mass Spectrometry-Data Independent Analysis (MS-DIAL) software version 4.60⁴² and R statistical environment Ver 4.0.5. Only metabolites present in 50% of the samples were measured, and metabolites whose coefficient of variation value was over 30% in pooled QC samples were removed from analysis. Annotation level 2 proposed by Schymanski et al.⁴³ was used for data analysis.

Histology. Back skin samples from control and IMQ-treated groups were collected and fixed in 10% formalin (FUJIFILM Wako Pure Chemical Corp., Tokyo, Japan). Staining with hematoxylin and eosin (HE) was performed at the Biopathology Institute Co., Ltd (Kunisaki, Oita, Japan) as previously reported²². Back skin samples were embedded in paraffin, and 3- μm sections were prepared and stained with HE. Representative images of two groups were obtained using a Keyence BZ-9000 Generation II microscope (Osaka, Japan) as previously reported²².

Quantitative real-time polymerase chain reaction. RNA was isolated using TRIzol LS Reagent (Invitrogen, Carlsbad, CA, USA) according to the manufacturer's instructions; cDNA was generated using the High-Capacity cDNA Reverse Transcription Kit (Applied Biosystems, Waltham, MA, USA) and TaKaRa polymerase chain reaction (PCR) Thermal Cycler Dice (Takara Bio Inc., Kusatsu, Shiga, Japan), and quantitative real-time PCR was performed using the StepOnePlus Real-Time PCR System (Applied Biosystems, Waltham, MA, USA). The mouse primers for glyceraldehyde-3-phosphate dehydrogenase (GAPDH) (4352339E), IL-17A (Mm00439618), and IL-23A (Mm00518984) were obtained from Applied Biosystems. The GAPDH housekeeping gene was used to normalize gene expression.

Statistical analysis. Data are shown as the mean \pm standard error of the mean. Data were analyzed using GraphPad Prism (Tokyo, Japan). Student's t-test was performed to compare spleen weights between the two groups. Spleen cell types and plasma metabolites were compared between the two groups using Mann-Whitney U-test with a false discovery rate (FDR) control. Correlations among spleen weight, spleen cells, and plasma metabolites were evaluated using Spearman's correlation analysis. For multivariate analysis of the metabolome data, orthogonal partial least squares discriminant analysis (OPLS-DA) was performed in Simca-P V.14.0 (Umetrics AB). Metabolites with VIP > 0.6 and *p*-value < 0.05 (Wilcoxon rank-sum test) were considered differentially abundant. Cumulative skin score, relative mRNA expression of skin, and body weight changes were analyzed with a Kruskal-Wallis test. *P* < 0.05 (or FDR-corrected *P* < 0.05) was considered statistically significant.

Data availability

The data that support the findings of this study are available from the corresponding author upon reasonable request.

Received: 9 March 2022; Accepted: 22 August 2022

Published online: 30 August 2022

References

- Mease, P. J. et al. Prevalence of rheumatologist – diagnosed psoriatic arthritis in patients with psoriasis in European/North American dermatology clinics. *J. Am. Acad. Dermatol.* **59**, 729–735. <https://doi.org/10.1016/j.jaad.2013.07.023> (2013).
- Ghoreschi, K., Balato, A., Enerbäck, C. & Sabat, R. Therapeutic targeting the IL-23 and IL-17 pathway in psoriasis. *Lancet* **397**, 754–766. [https://doi.org/10.1016/S0140-6736\(21\)00184-7](https://doi.org/10.1016/S0140-6736(21)00184-7) (2021).
- Griffiths, C. E. M., Armstrong, A. W., Gudjonsson, J. E. & Barker, J. N. W. N. Psoriasis. *Lancet* **397**(10281), 1301–1315. [https://doi.org/10.1016/S0140-6736\(20\)32549-6](https://doi.org/10.1016/S0140-6736(20)32549-6) (2021).
- Sharma, A. et al. IL-23/Th17 axis: A potential therapeutic target for psoriasis. *Curr. Drug Res. Rev.* **14**, 24–36. <https://doi.org/10.2174/2589977513666210707114520> (2022).
- Nestle, F. O., Kaplan, D. H. & Barker, J. Psoriasis. *N. Engl. J. Med.* **361**, 496–509. <https://doi.org/10.1056/NEJMra0804595> (2009).
- Boehncke, W. H. & Schön, M. P. Psoriasis. *Lancet* **386**, 983–994. [https://doi.org/10.1016/S0140-6736\(14\)61909-7](https://doi.org/10.1016/S0140-6736(14)61909-7) (2015).
- Rendon, A. & Schäkel, K. Psoriasis pathogenesis and treatment. *Int. J. Mol. Sci.* **20**, 1475. <https://doi.org/10.3390/ijms20061475> (2019).
- Armstrong, A. W. & Read, C. Pathophysiology, clinical presentation, and treatment of psoriasis: A review. *JAMA* **323**, 1945–1960. <https://doi.org/10.1001/jama.2020.4006> (2020).

9. van der Fits, L. *et al.* Imiquimod-induced psoriasis-like skin inflammation in mice is mediated via the IL-23/IL-17 axis. *J. Immunol.* **182**, 5836–5845. <https://doi.org/10.4049/jimmunol.0802999> (2009).
10. Flutter, B. & Nestle, F. O. TLRs to cytokines: Mechanistic insights from the imiquimod mouse model of psoriasis. *Eur. J. Immunol.* **43**, 3138–3146. <https://doi.org/10.1002/eji.201343801> (2013).
11. Slominski, A. & Wortsman, J. Neuroendocrinology of the skin. *Endocr. Rev.* **21**, 457–487. <https://doi.org/10.1210/edrv.21.5.0410> (2000).
12. Slominski, A. T., Manna, P. R. & Tuckey, R. C. On the role of skin in the regulation of local and systemic steroidogenic activities. *Steroids* **103**, 72–88. <https://doi.org/10.1016/j.steroids.2015.04.006> (2015).
13. Qin, S. *et al.* Endogenous n-3 polyunsaturated fatty acids protect against imiquimod-induced psoriasis-like inflammation via the IL-17/IL-23 axis. *Mol. Med. Rep.* **9**, 2097–2104. <https://doi.org/10.3892/mmr.2014.2136> (2014).
14. Huang, S. W. *et al.* Azithromycin impairs TLR7 signaling in dendritic cells and improves the severity of imiquimod-induced psoriasis-like skin inflammation in mice. *J. Dermatol. Sci.* **84**, 59–70. <https://doi.org/10.1016/j.jdermsci.2016.07.007> (2016).
15. Lee, J. *et al.* Tussilagonone ameliorates psoriatic features in keratinocytes and imiquimod-induced psoriasis-like lesions in mice via NRF2 activation. *J. Invest. Dermatol.* **140**, 1223–1232. <https://doi.org/10.1016/j.jid.2019.12.008> (2020).
16. Schwarz, A., Philippsen, R. & Schwarz, T. Induction of regulatory T cells and correction of cytokine imbalance by short-chain fatty acids: Implications for psoriasis therapy. *J. Invest. Dermatol.* **141**, 95–104. <https://doi.org/10.1016/j.jid.2020.04.031> (2021).
17. Zhang, S. *et al.* Hyperforin ameliorates imiquimod-induced psoriasis-like murine skin inflammation by modulating IL-17A-producing gammadelta T cells. *Front. Immunol.* **12**, 635076. <https://doi.org/10.3389/fimmu.2021.635076> (2021).
18. Mebius, R. E. & Kraal, G. Structure and function of the spleen. *Nat. Rev. Immunol.* **5**, 606–616. <https://doi.org/10.1038/nri1669> (2005).
19. Bronte, V. & Pittel, M. J. The spleen in local and systemic regulation of immunity. *Immunity* **39**, 806–818. <https://doi.org/10.1016/j.immuni.2013.10.010> (2013).
20. Lewis, S. M., Williams, A. & Eisenbarth, S. C. Structure and function of the immune system in the spleen. *Sci. Immunol.* **4**, eaau6085. <https://doi.org/10.1126/sciimmunol.aau6085> (2019).
21. Wei, Y. *et al.* Brain - spleen axis in health and diseases: A review and future perspective. *Brain Res. Bull.* **182**, 130–140. <https://doi.org/10.1016/j.brainresbull.2022.02.008> (2022).
22. Shinno-Hashimoto, H. *et al.* Abnormal composition of microbiota in the gut and skin of imiquimod-treated mice. *Sci. Rep.* **11**, 11265. <https://doi.org/10.1038/s41598-021-90480-4> (2021).
23. Balato, N. *et al.* Nonalcoholic fatty liver disease, spleen and psoriasis: New aspects of low-grade chronic inflammation. *World J. Gastroenterol.* **21**, 6892–6897. <https://doi.org/10.3748/wjg.v21.i22.6892> (2015).
24. Di, T. *et al.* Study on the effect of spleen deficiency on the pathogenesis of psoriasis based on intestinal microbiome. *Longhua Chin. Med.* **2**, 14 (2019).
25. Marcinkiewicz, J. & Kontny, E. Taurine and inflammatory diseases. *Amino Acids* **46**, 7–20. <https://doi.org/10.1007/s00726-012-1361-4> (2014).
26. Niu, X., Zheng, S., Liu, H. & Li, S. Protective effects of taurine against inflammation, apoptosis, and oxidative stress in brain injury. *Mol. Med. Rep.* **18**, 4516–4522. <https://doi.org/10.3892/mmr.2018.9465> (2018).
27. Ottas, A. *et al.* The metabolic analysis of psoriasis identifies the associated metabolites while providing computational models for the monitoring of the disease. *Arch. Dermatol. Res.* **309**, 519–528. <https://doi.org/10.1007/s00403-017-1760-1> (2017).
28. Vahdat, M. *et al.* The effects of Taurine supplementation on inflammatory markers and clinical outcomes in patients with traumatic brain injury: A double-blind randomized controlled trial. *Nutr. J.* **20**, 53. <https://doi.org/10.1186/s12937-021-00712-6> (2021).
29. Lightowler, L. E. & Rylance, H. J. Substituted dihydroxybenzoic acids as possible anti-inflammatory agents. *J. Pharm. Pharmacol.* **15**, 633–638 (1963).
30. Smith, K. G. & Hunt, J. L. On the use of spleen mass as a measure of avian immune system strength. *Ecophysiology* **138**, 28–31. <https://doi.org/10.1007/s00442-003-1409-y> (2004).
31. Zhang, J. *et al.* A key role of the subdiaphragmatic vagus nerve in the depression-like phenotype and abnormal composition of gut microbiota in mice after lipopolysaccharide administration. *Transl. Psychiatry* **10**, 186. <https://doi.org/10.1038/s41398-020-00878-3> (2020).
32. Zhang, J. *et al.* (R)-Ketamine attenuates LPS-induced endotoxin-derived delirium through inhibition of neuroinflammation. *Psychopharmacology* **238**, 2743–2753. <https://doi.org/10.1007/s00213-021-05889-6> (2021).
33. Ma, L. *et al.* Nuclear factor of activated T cells 4 in the prefrontal cortex is required for prophylactic actions of (R)-ketamine. *Transl. Psychiatry* **12**, 27. <https://doi.org/10.1038/s41398-022-01803-6> (2022).
34. Zhang, K. *et al.* Splenic NKG2D confers resilience versus susceptibility in mice after chronic social defeat stress: Beneficial effects of (R)-ketamine. *Eur. Arch. Psychiatry Clin. Neurosci.* **271**, 447–456. <https://doi.org/10.1007/s00406-019-01092-z> (2021).
35. Hashimoto, K. Molecular mechanisms of the rapid-acting and long-lasting antidepressant actions of (R)-ketamine. *Biochem. Pharmacol.* **177**, 113935. <https://doi.org/10.1016/j.bcp.2020.113935> (2020).
36. Wei, Y., Chang, L. & Hashimoto, K. Molecular mechanisms underlying the antidepressant actions of arketamine: Beyond the NMDA receptor. *Mol. Psychiatry* **27**, 559–573. <https://doi.org/10.1038/s41380-021-01121-1> (2022).
37. Walter, A. *et al.* Aldara activates TLR7-independent immune defence. *Nat. Commun.* **4**, 1560. <https://doi.org/10.1038/ncomms2566> (2013).
38. Flutter, B. & Nestle, F. O. TLRs to cytokines: Mechanistic insights from the imiquimod mouse model of psoriasis. *Eur. J. Immunol.* **43**, 3138–3146. <https://doi.org/10.1002/eji.201343801> (2013).
39. Wei, Y. *et al.* Abnormalities of the composition of the gut microbiota and short-chain fatty acids in mice after splenectomy. *Brain Behav. Immun. Health* **11**, 100198. <https://doi.org/10.1016/j.bbih.2021.100198> (2021).
40. Wan, X. *et al.* Effects of (R)-ketamine on reduced bone mineral density in ovariectomized mice: A role of gut microbiota. *Neuropharmacology* **213**, 109139. <https://doi.org/10.1016/j.neuropharm.2022.109139> (2022).
41. Wan, X. *et al.* Gut-microbiota-brain axis in the vulnerability to psychosis in adulthood after repeated cannabis exposure during adolescence. *Eur. Arch. Psychiatry Clin. Neurosci.* <https://doi.org/10.1007/s00406-022-01437-1> (2022).
42. Tsugawa, H. *et al.* MS-DIAL: Data-independent MS/MS deconvolution for comprehensive metabolome analysis. *Nat. Methods* **12**, 523–526. <https://doi.org/10.1038/nmeth.3393> (2015).
43. Schymanski, E. L. *et al.* Identifying small molecules via high resolution mass spectrometry: Communicating confidence. *Environ. Sci. Technol.* **48**, 2097–2098. <https://doi.org/10.1021/es5002105> (2014).

Acknowledgements

This study was in part supported by JST OPERA Program Japan (to C.M JPMJOP1831) and unrestricted grant of Yamada Bee Company, Japan (to C.M).

Author contributions

H.S.H. conceived the project, designed the experiments, analyzed the data, and drafted the manuscript. H.S.H., X.W., Y.H., and Y.F. performed the experiments. A.E. and C.M. performed metabolomics analysis. H.S.H., A.S.,

and M.H. performed flow cytometry analysis of spleen. C.M., M.H., and K.H. worked on the general coordination of the study. K.H. conceived the project, designed the experiments, and wrote the manuscript.

Competing interests

The authors declare no competing interests.

Additional information

Correspondence and requests for materials should be addressed to H.S.-H. or K.H.

Reprints and permissions information is available at www.nature.com/reprints.

Publisher's note Springer Nature remains neutral with regard to jurisdictional claims in published maps and institutional affiliations.



Open Access This article is licensed under a Creative Commons Attribution 4.0 International License, which permits use, sharing, adaptation, distribution and reproduction in any medium or format, as long as you give appropriate credit to the original author(s) and the source, provide a link to the Creative Commons licence, and indicate if changes were made. The images or other third party material in this article are included in the article's Creative Commons licence, unless indicated otherwise in a credit line to the material. If material is not included in the article's Creative Commons licence and your intended use is not permitted by statutory regulation or exceeds the permitted use, you will need to obtain permission directly from the copyright holder. To view a copy of this licence, visit <http://creativecommons.org/licenses/by/4.0/>.

© The Author(s) 2022